Lawrence Berkeley National Laboratory
Recent Work

Title
ORTHOGONAL DISPERSION SPECTROMETER FOR MISSING MASS SPECTRA

Permalink
https://escholarship.org/uc/item/5m25489q

Authors
Ankenbrandt, C.M.
Clark, A.R.
Cork, Bruce
et al.

Publication Date
1965-05-06

eScholarship.org Powered by the California Digital Library
University of California

UCRL-11995

University of California

Ernest O. Lawrence Radiation Laboratory

TWO-WEEK LOAN COPY

This is a Library Circulating Copy which may be borrowed for two weeks. For a personal retention copy, call Tech. Info. Division, Ext. 5545

ORTHOGONAL DISPERSION SPECTROMETER FOR MISSING MASS SPECTRA

Berkeley, California

DISCLAIMER

This document was prepared as an account of work sponsored by the United States Government. While this document is believed to contain correct information, neither the United States Government nor any agency thereof, nor the Regents of the University of California, nor any of their employees, makes any warranty, express or implied, or assumes any legal responsibility for the accuracy, completeness, or usefulness of any information, apparatus, product, or process disclosed, or represents that its use would not infringe privately owned rights. Reference herein to any specific commercial product, process, or service by its trade name, trademark, manufacturer, or otherwise, does not necessarily constitute or imply its endorsement, recommendation, or favoring by the United States Government or any agency thereof, or the Regents of the University of California. The views and opinions of authors expressed herein do not necessarily state or reflect those of the United States Government or any agency thereof or the Regents of the University of California.

UCRL-11995

UNIVERSITY OF CALIFORNIA

Lawrence Radiation Laboratory
Berkeley, California

AEC Contract No. W-7405-eng-48

ORTHOGONAL DISPERSION SPECTROMETER FOR MISSING MASS SPECTRA

C. M. Ankenbrandt, A. R. Clark, Bruce Cork,
T. Elioff, L. T. Kerth, and W. A. Wenzel

May 6, 1965

(For presentation at the Purdue Instrumentation Conference
May 12-14, 1965)

ORTHOGONAL DISPERSION SPECTROMETER FOR MISSING MASS SPECTRA

C. M. Ankenbrandt, A. R. Clark, Bruce Cork,
T. Elioff, L. T. Kerth, and W. A. Wenzel

Lawrence Radiation Laboratory
University of California
Berkeley, California

May 6, 1965

ABSTRACT

For interactions of the type $M_1 + M_2 \rightarrow M_3 + M_4$ the kinematics of both initial particles and one secondary particle determine the reaction completely. Given a fixed initial state and any missing mass M_4, the momentum–angle correlation for particle M_3 is determined uniquely. In the spectrometer described, this correlation is preserved as a line image in the focal plane of a double focusing magnetic lens. Dispersions both in the plane of production and at right angles to it separate the images corresponding to different values of M_4, for which the spectrum is obtained directly by means of a 28–counter hodoscope in the focal plane. Each hodoscope counter is gated with a scintillation and Čerenkov counter telescope to identify particle M_3. During each beam pulse the outputs from the hodoscope counters are recorded on 10 Mc/sec scalers. Between accelerator pulses the contents of these scalers are read onto magnetic tape and into a PDP–5 computer, which accumulates, corrects, and displays the data continuously to provide an on–line monitor.

I. INTRODUCTION

Most of the many known elementary particles are unstable. Such particles are often identified from the measurements of correlated decay secondaries produced in high energy interactions. The measurement of mass spectra with bubble chambers is now common, and recently the use with magnetic analysis of sets of either counter hodoscopes or spark chambers has become widespread. The apparatus described in this report is a comparatively high resolution spectrometer designed to take advantage of the high intensity and relatively good optical quality of the Bevatron external proton beam.

For reactions of the type

$$M_1 + M_2 \rightarrow M_3 + M_4 \tag{1}$$

masses of both stable and unstable particles may be determined from "missing mass" measurements, in which the initial state is kinematically well defined, and the angle and momentum of one of the final state particles, say M_3, is measured. In terms of the momentum and energy of M_1, M_2, and M_3 the mass M_4 is given by

$$M_4^2 = (E_1 + E_2 - E_3)^2 - (\vec{P} + \vec{P}_2 - \vec{P}_3)^2 \tag{2}$$

or

$$M_4^2 = M_1^2 + M_2^2 + M_3^2 + 2 E_1 M_2 - 2 E_3 (M_2 + E_1) + 2 P_1 P_3 \cos \theta_3 \tag{3}$$

where M_2 is assumed to be at rest, and θ_3 measures the laboratory angle between $\vec{P}_3$ and the incident momentum $\vec{P}_1$.

II. PROPERTIES OF THE SPECTROMETER

A. General Optical Properties

Figure 1 shows the optical properties of the spectrometer in a schematic way. The incident beam is made parallel in the plane of production and is well focussed at the target in the plane orthogonal to the plane of production. Regardless of target size, secondary particles of a given momentum P_3 are focussed in the plane of production to a point whose position depends uniquely on the angle of production θ_3. Similarly in a plane at right angles to the production plane the particles are dispersed according to momentum; and an image of the (approximate) point source at the target is produced.

For a given M_1, M_2, M_3, M_4, and $\vec{P}_1$, the total image formed in the x,y plane (Fig. 2) is a line. In the limit that the kinematic variables change linearly across the aperture, this line is straight and at an angle δ to the x-axis. This angle of "chromatic rotation" is given by

$$\cot \delta = \left[X - F P_3 \left(\partial\theta_3/\partial P_3\right)_{M_4} \right] / Y \qquad (4)$$

where we define

$$X \equiv P_3(\partial x/\partial P_3)_{\theta_3}; \; Y \equiv P_3(\partial y/\partial P_3)_{M_4} \equiv P_3 (dy/dP_3); \quad F \equiv (\partial x/\partial\theta_3)_{P_3}$$

Substituting from (3) into (4) we obtain

$$\cot \delta = \left\{ X + F[(\beta_3/P_1) (E_1 + M_2) \csc \theta_3 - \cot \theta_3] \right\} / Y \qquad (5)$$

Given the identification of secondary particle M_3 a line detector in the image plane (Fig. 2) determines M_4 uniquely. The minimum mass width (neglecting Coulomb scattering and aberrations) for a detector of nonzero width is given in terms of the rate of mass change in the direction normal to the detector.

For a detector of width W, this resolution is

$$\Delta M_4^2 = (W/F)\ (\partial M_4^2/\partial \theta)_p \csc \delta = 2\ P_1\ P_3\ (W/F) \sin \theta_3 \csc \delta \qquad (6)$$

In practical cases the effective mass resolution is worsened because of incident beam divergence, energy spread, and source size, as well as by Coulomb scattering and magnet aberrations. Chromatic aberration is important when the momentum spread at the detector is more than a few percent.

B. Experimental Spectrometers

Two experimental arrangements which have employed orthogonal dispersion spectrometers at the Bevatron are shown in Figs. 3 and 4, respectively. In the system shown in Fig. 3[1,2] either of two channels used a target movable along the beam line. The high momentum channel had an aperture of about 10^{-3} steradians and accepted production angles from 25 to 80 degrees and momenta from 0.4 to 4 GeV/c. For the low momentum channel the aperture was 10^{-2} steradians, the angular range 50–90 degrees, and the momentum range 0.06 – 0.6 GeV/c.

The remainder of this report deals with the spectrometer shown in Fig. 4 for which the target was fixed, while magnets B_1 and B_2 were moved to change the production angle. This latter arrangement was particularly suitable for use with the liquid hydrogen or deuterium target, which would have been relatively difficult to move over the required distance. Secondary particles with momenta up to 7 GeV/c and laboratory angles from 9.5 to 70 degrees were detected with an aperture of 10^{-4} steradians. B_1 and B_2 moved along a steel plate using 24 in. diameter "Hovair" pads — four to each magnet — operated at an air pressure of 30 psi and a total flow of 100 ft^3/min NTP. The motion was remotely controlled, and guide rails insured proper relative alignment of the magnets. Bellows-type helium bags moved with the magnets to provide a low-scattering path for the beam. B_1, B_2, and B_3 were uniform field magnets that produced no focussing in the plane of production, and the dispersion in y resulted from a small angle deflection (15 degrees). Hence we may write

$X = -F\ (\theta_c - \theta_3)$ and $Y \approx -H$ (see Fig. 1), so that (5) becomes simply

$$\cot \delta = (F/H)\ [\theta_c - \theta_3 + \cot \theta_3 - (\beta_3/P_1)\ (E_1 + M_2) \csc \theta_3] \qquad (7)$$

III. DETECTION SYSTEM

A. Counter Arrangement

In spite of the respectable aperture and large mass width acceptable under most conditions, the relevant kinematical information is preserved in

the image plane. Hence the entire detection system can be well shielded from the large background associated with the production target. Instantaneous incident fluxes of order 10^{12} protons per second have been used.

The detection system included gas Čerenkov counters C_1, C_2, and C_3, together with a water Čerenkov counter and several scintillators. These were used in various combinations to identify different secondaries as required for reactions of the types

$$P + P \rightarrow M_3 + M_4$$

and (8)

$$P + D \rightarrow M_3 + M_4$$

where M_3 = P, π, K, D, etc.

The 28 element scintillation counter hodoscope (Fig. 2), for which each counter had a sensitive area 7–in. x 1/4–in. and a thickness 1/2–in. in the beam direction, could be rotated by remote control to provide any required angle of chromatic rotation, δ.

B. Electronics and On–Line Computer

Figure 5 shows a block diagram of the electronics used to identify particle M_3, to store the hodoscope information, and to assimilate and display the data using an on–line Digital Equipment Corporation PDP–5 computer. The pulses from each hodoscope counter were gated with a signal from the circuitry which identified particle M_3. The gated pulses were scaled on 10 Mc/sec scalers with capacity 10^3 counts. Between Bevatron pulses these were interrogated and reset by the computer, and the contents

were both recorded on magnetic tape and accumulated in the computer memory. Other information recorded on a pulse-to-pulse basis included total channel flux, beam intensity (from an ion chamber), and pulse number. Additional information recorded at the beginning of each run included magnet currents, run number, calibration data, etc.

Additional functions performed by the computer included:

1. Retention of accumulated data from the preceeding as well as the current run, and recall of earlier data from magnetic tape for checking and comparison.
2. Calculation of a polynomial fit (up to 4th order) to the hodoscope data.
3. Calculation of first or second differences from the hodoscope data.
4. Systematic correction of hodoscope data according to a given pattern or one derived from operational data, including the normalization of hodoscope data to beam intensity.
5. Calculation of statistical errors for the accumulated data.
6. Control of display oscilloscope.

A very important function of the computer was the control of an on-line display oscilloscope which could be used to present the raw, accumulated, or corrected data. A typical computer display scope pattern is shown in Fig. 6. The vertical scale was adjusted automatically to keep the pattern compatible with the available display area. The first six positions on the left indicate scale factors, the two positions on the extreme right show the statistical error for the fourteenth hodoscope counter. The time

required for accumulation of the necessary data was about 100 ms per accelerator cycle; ordinarily an equal amount of time was required for computation. Hence the oscilloscope display, including pulse by pulse correction, was effectively continuous.

Following each completed run the accumulated data were typed out, and a polaroid photograph of the display oscilloscope was made. Figure 7 shows the combined data from six runs, showing how relatively small peaks may be identified above background. The immediately accessible record provided by the oscilloscope photographs was very useful for making consistency checks in a series of runs, and for rapid interpretation of the effects of changes in operating conditions.

IV. MEASUREMENT PRECISION

The hodoscope provided a momentum resolution as good as 0.4%, corresponding to a 1/4-in. counter with vertical dispersion $H \approx 60$-in. at $\delta = 0$. The precision of any measurement depends upon the primary as well as the secondary momentum. To control the energy of the Bevatron external beam a gate was generated whenever the magnetic field of the accelerator fell between two preset limits differing by 0.4%. In this way the scalers were gated only when the beam energy was correct. In general a reduction of about 30% in beam efficiency occurred because of timing jitters in the start of the flattop. In most cases a beam spill of order 0.5 second was obtained. Another source of error was introduced by beam divergence or steering drift.

This angular error is estimated to be less than 1 mr. The vertical source size was about 1/4–in., but this was demagnified by nearly a factor of two at the image plane. That the central resolution was approximately as expected is indicated in Fig. 6, which shows elastically scattered protons contained almost entirely within a single hodoscope counter. Any improvement in resolution attainable with spark chambers would have been small. The higher data rate and easier data handling for counters was particularly important in this application.

For recording missing mass spectra the most important advantage of the hodoscope over a single counter lies not so much in the increased data rate but in the insensitivity of the distribution pattern involving all counters to fluctuations in targetting efficiency, beam steering, etc. This feature in particularly important in the search for small "bumps" above a large background. It was determined in statistically significant tests that the detection efficiencies of the counters could be relatively "plateaued" to within a few tenths of one percent.

ACKNOWLEDGMENTS

The authors are indebted to A. R. Clyde, D. Keefe, and W. M. Layson, who collaborated in the early part of the work described here.

REFERENCES

1. A. R. Clyde, Bruce Cork, D. Keefe, L. T. Kerth, W. M. Layson, and W. A. Wenzel, Proton-Proton Elastic Scattering, UCRL-11441, July 1964, presented at Int. Conf. on High Energy Physics, Dubna, USSR, August 5-15, 1964.

2. C. M. Ankenbrandt, A. R. Clyde, Bruce Cork, D. Keefe, L. T. Kerth, W. M. Layson, and W. A. Wenzel, Production of Nucleon Isobars by 7.1 GeV/c Protons, UCRL-11423 (Revised), July 1964, presented at Int. Conf. on High Energy Physics, Dubna, USSR, August 5-15, 1964; also Nuovo Cimento 35, 1052 (1965).

FIGURE CAPTIONS

Fig. 1 Schematic of the optical properties of the orthogonal dispersion spectrometer. Details of operation are given in the text.

Fig. 2 Image plane of the spectrometer showing 28 element counter hodoscope rotated through angle δ determined by horizontal and vertical dispersions and by production kinematics.

Fig. 3 Experimental arrangement showing two spectrometers used in the Bevatron external proton beam. (References 1 and 2)

Fig. 4 Experimental arrangement showing the spectrometer used with 28 element counter hodoscope and flexible particle identification system.

Fig. 5 Block diagram of the electronics used with the experimental arrangement shown in Fig. 4.

Fig. 6 Photograph of computer controlled display oscilloscope for experimental arrangement of Fig. 4. P_1 = 5.0 BeV/c, M_1 = 938 MeV/c^2, θ_3 = 10.5 deg, M_3 = 938 MeV/c^2. The position of the peak is at M_4 = 938 MeV/c^2 (p–p elastic scattering). Each counter corresponds to a mass width of 22 MeV/c^2.

Fig. 7 Combined patterns from six adjoining mass ranges for the reaction $P + P \rightarrow P + N^*$.

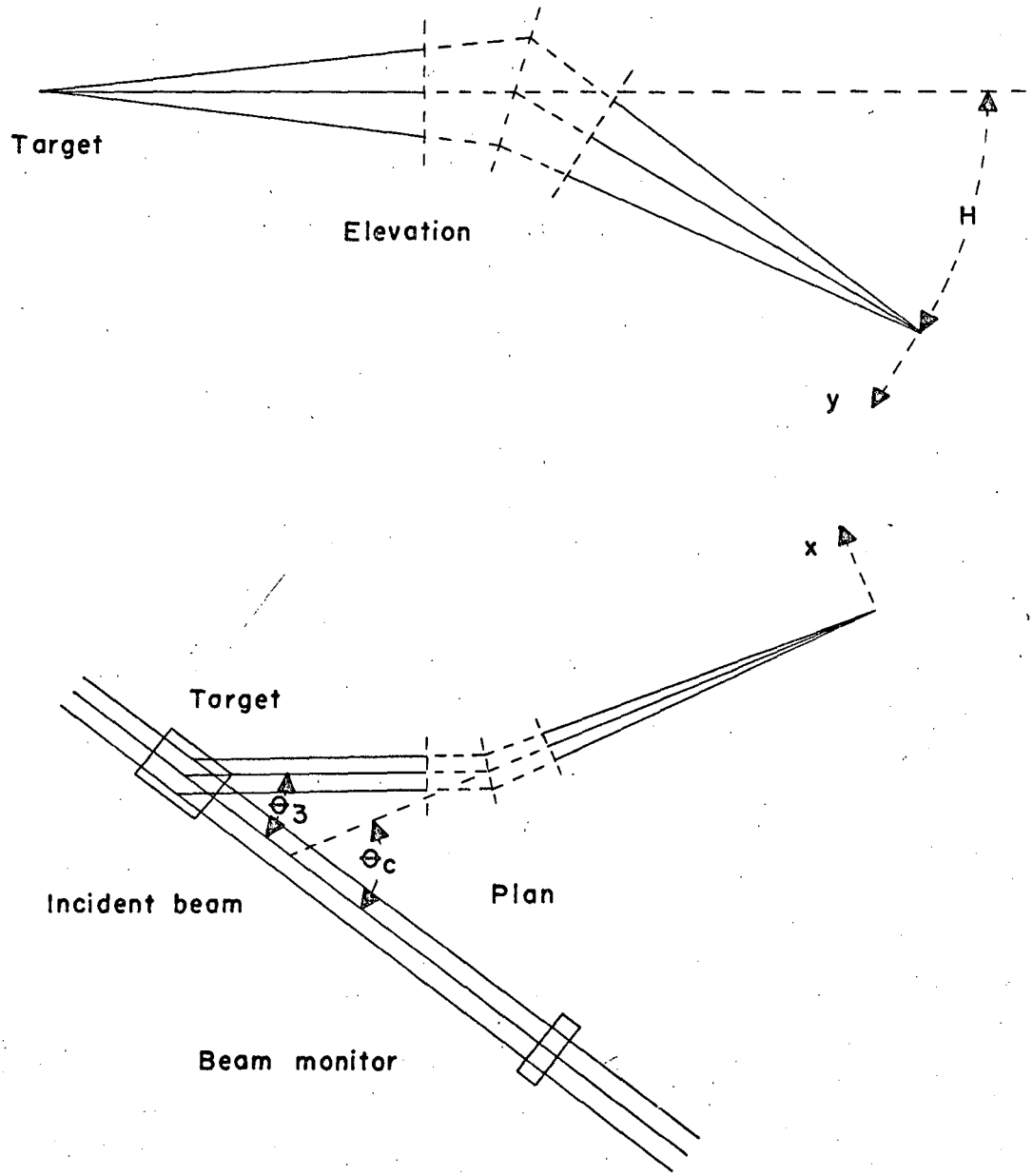

MUB-5976

Fig. 1

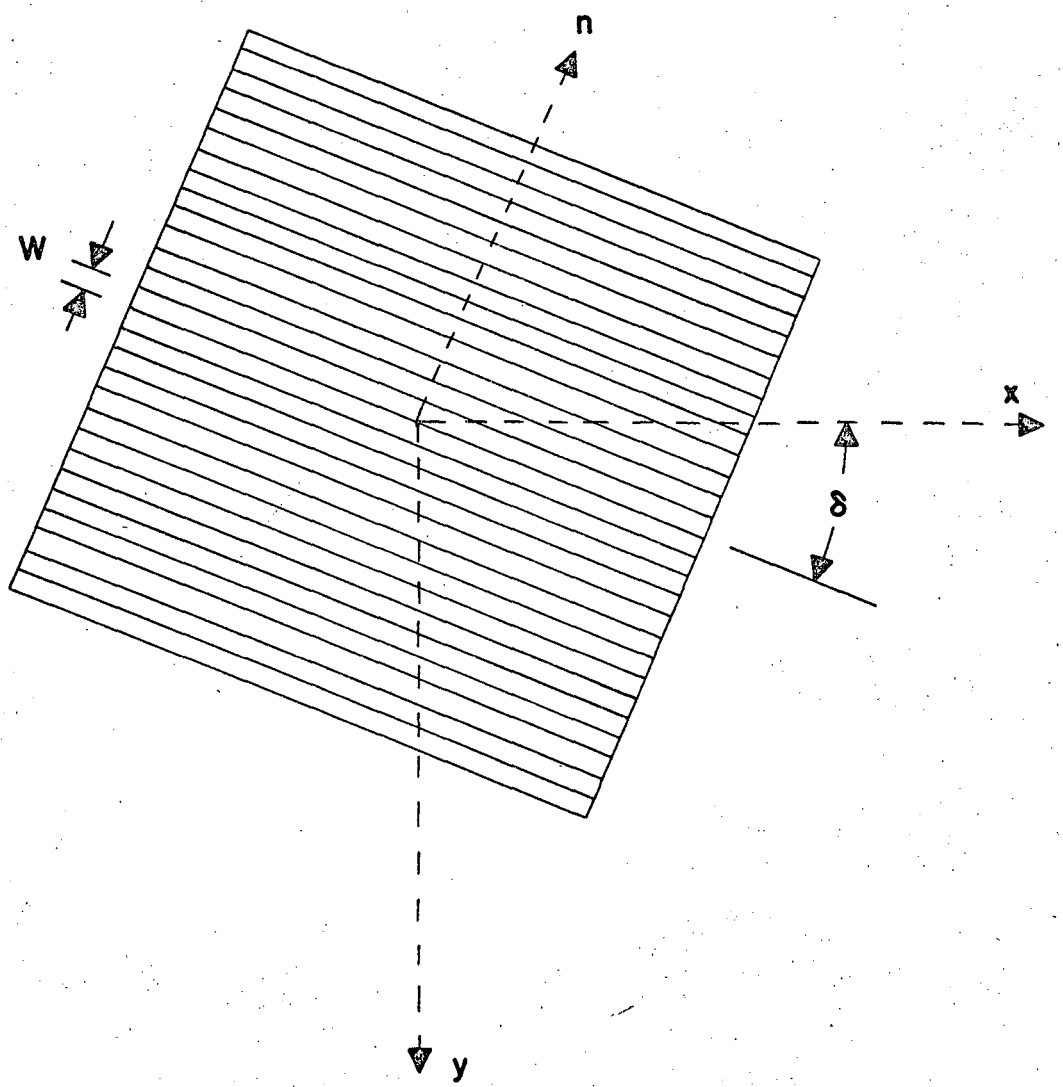

MUB-5977

Fig. 2

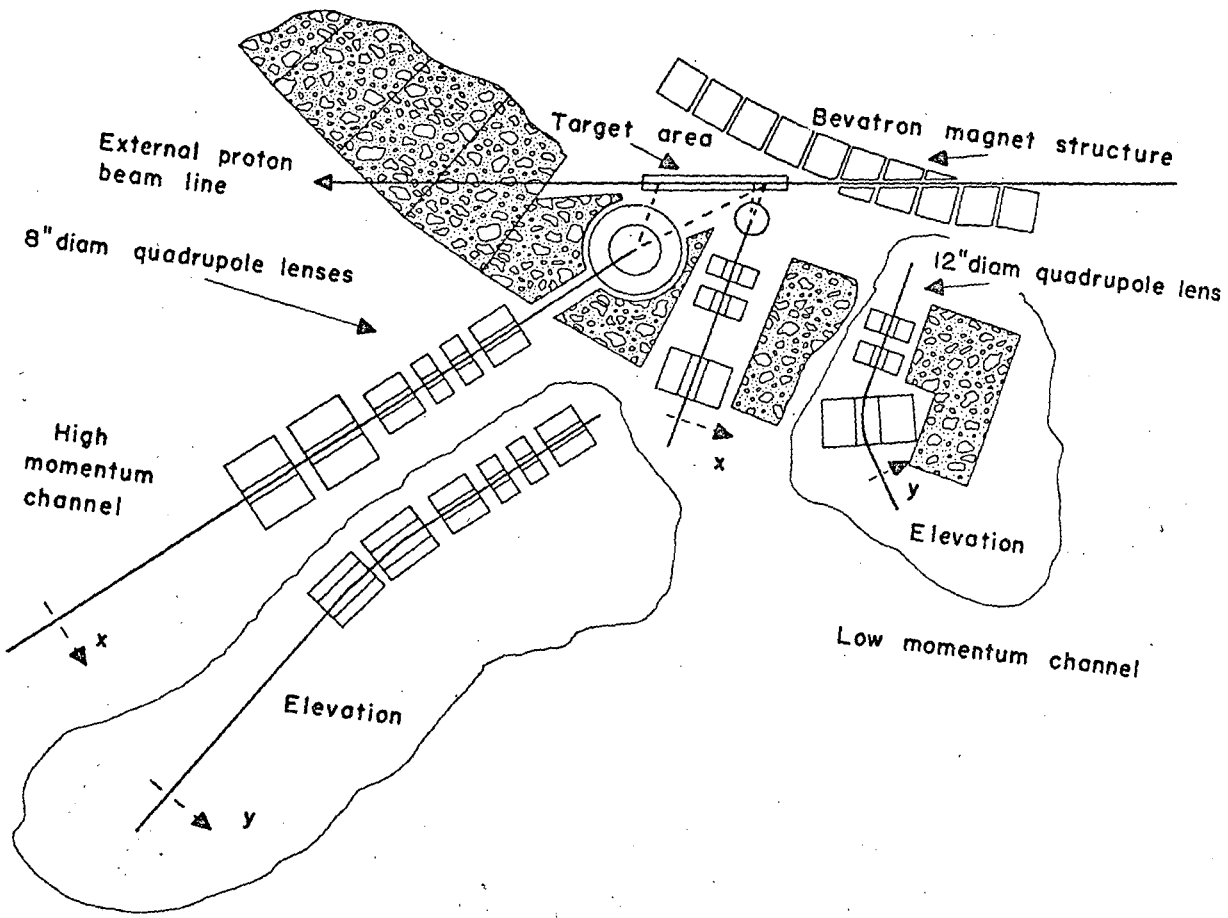
External proton
beam line
Target area
Bevatron magnet structure
8"diam quadrupole lenses
12"diam quadrupole lens
High
momentum
channel
x
y
Elevation
x
y
Elevation
Low momentum channel
MUB-5978

Fig. 3

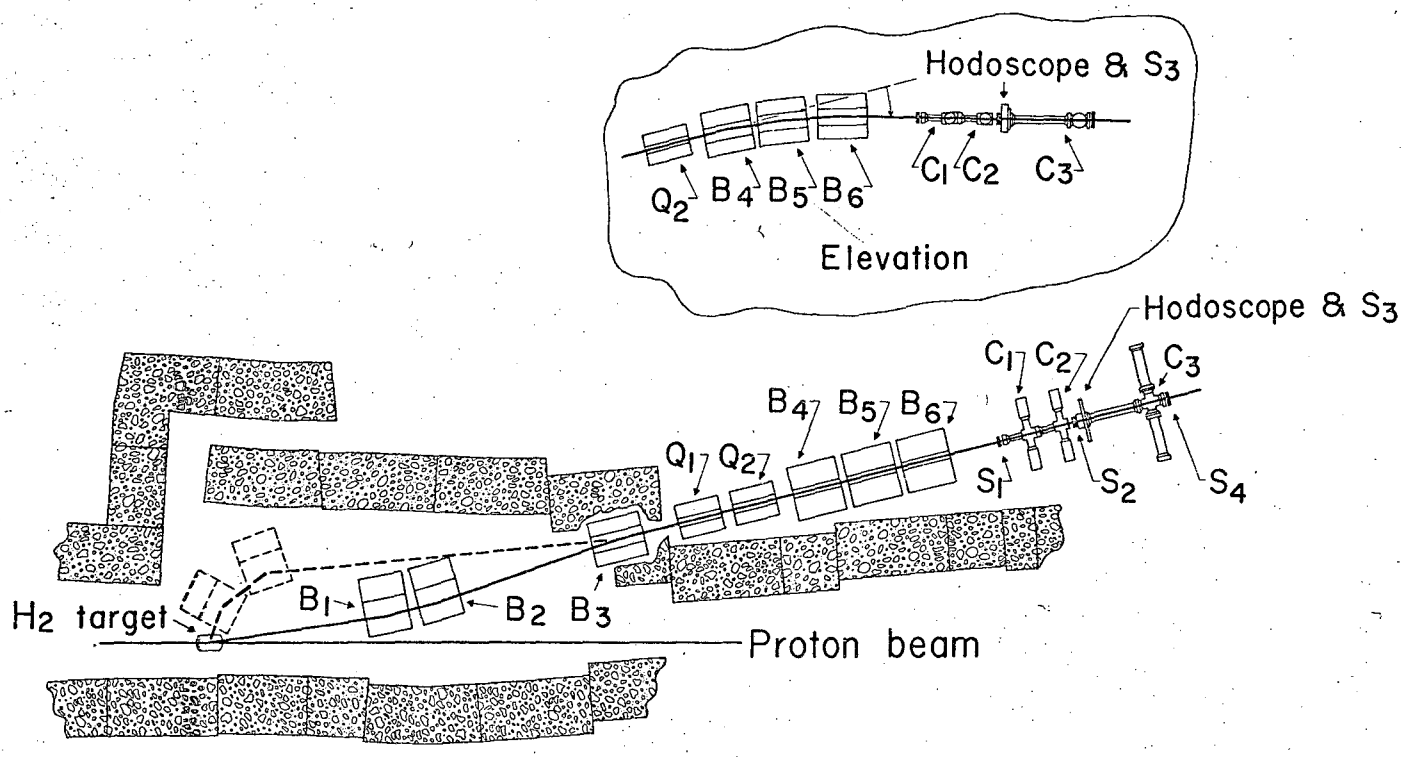
Hodoscope & S3
C1 C2 C3
Q2 B4 B5 B6
Elevation
Hodoscope & S3
C1 C2 C3
B4 B5 B6
Q1 Q2
S1
S2
S4
B1
B2 B3
H2 target
Proton beam
MUB-5979

Fig. 4

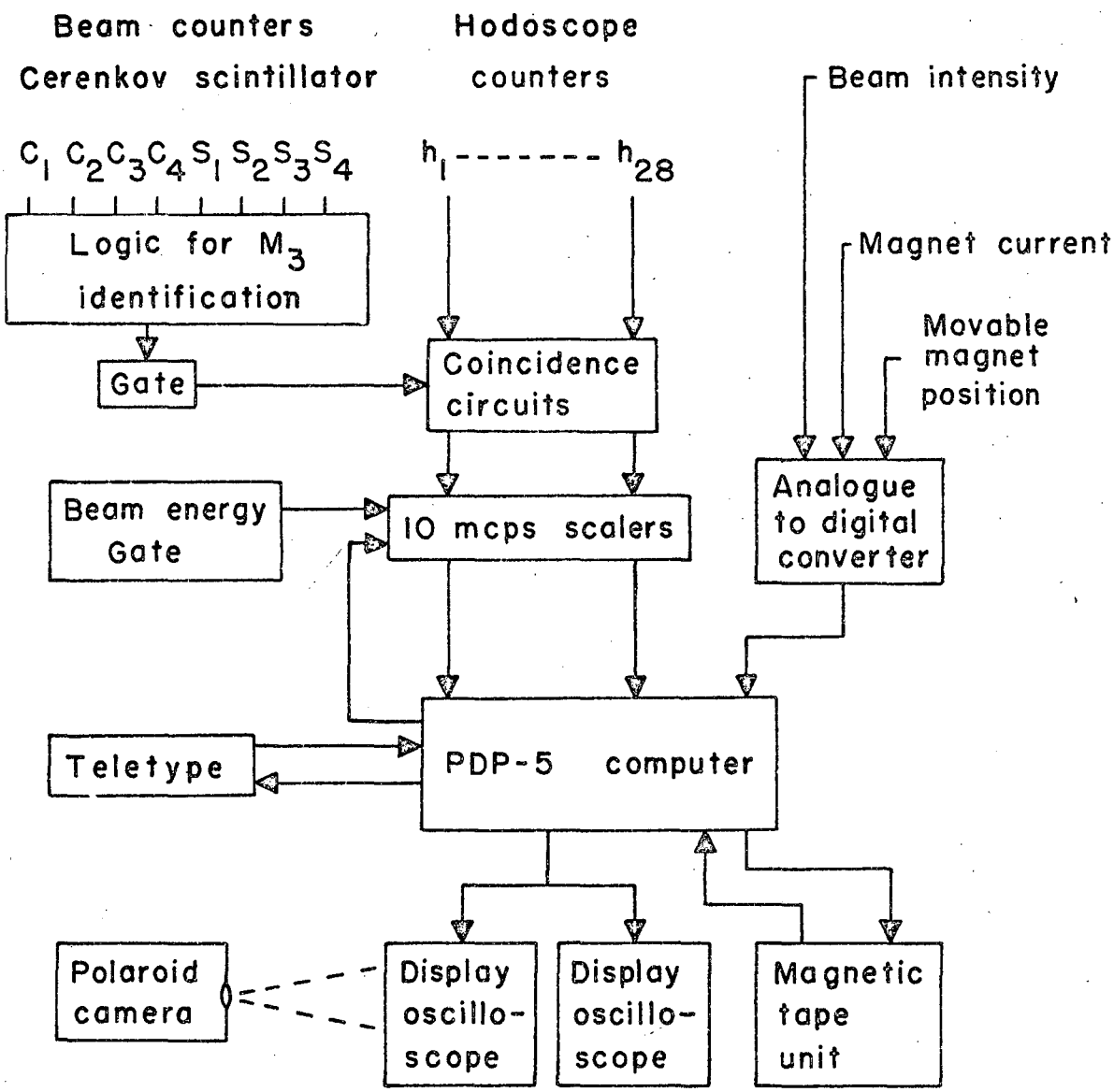

MUB-5980

Fig. 5

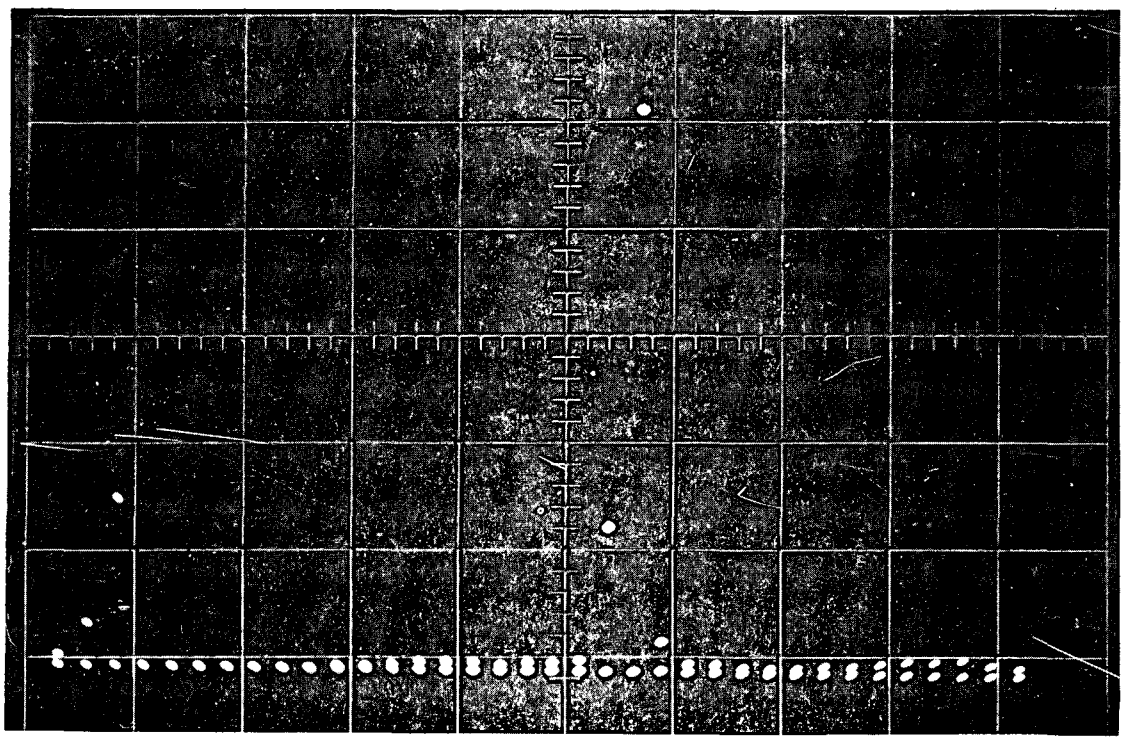

ZN-4909

Fig. 6

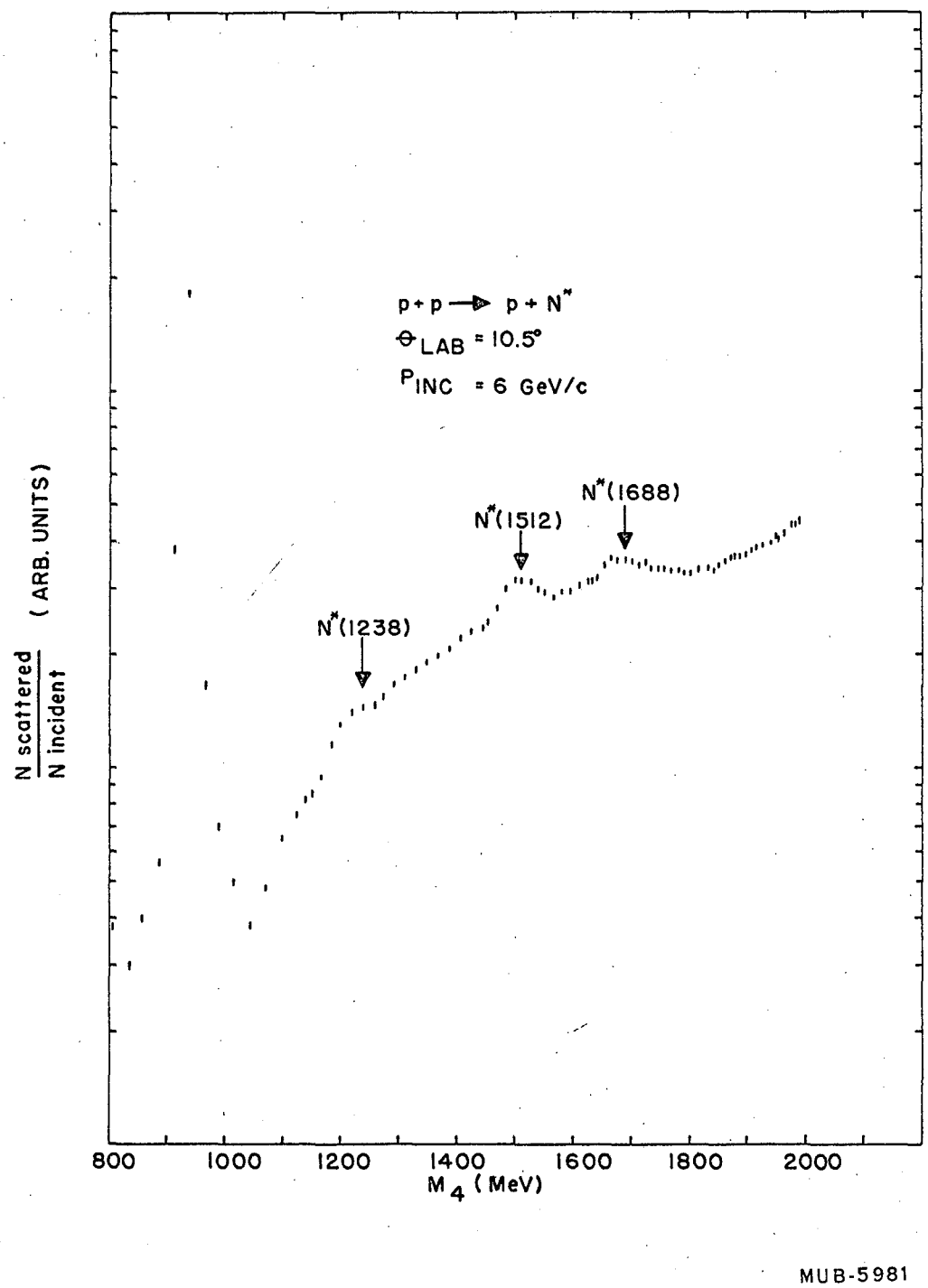
p + p → p + N*
θ LAB = 10.5°
P INC = 6 GeV/c
N*(1238)
N*(1512)
N*(1688)
N scattered / N incident (ARB. UNITS)
800
1000
1200
1400
1600
1800
2000
M 4 (MeV)
MUB-5981

Fig. 7

This report was prepared as an account of Government sponsored work. Neither the United States, nor the Commission, nor any person acting on behalf of the Commission:

A. Makes any warranty or representation, expressed or implied, with respect to the accuracy, completeness, or usefulness of the information contained in this report, or that the use of any information, apparatus, method, or process disclosed in this report may not infringe privately owned rights; or

B. Assumes any liabilities with respect to the use of, or for damages resulting from the use of any information, apparatus, method, or process disclosed in this report.

As used in the above, "person acting on behalf of the Commission" includes any employee or contractor of the Commission, or employee of such contractor, to the extent that such employee or contractor of the Commission, or employee of such contractor prepares, disseminates, or provides access to, any information pursuant to his employment or contract with the Commission, or his employment with such contractor.